Two Size-Selective Mechanisms Specifically Trap Bacteria-Sized Food Particles in Caenorhabditis elegans

Two size-selective mechanisms specifically trap bacteria-sized food particles in *Caenorhabditis elegans*

Christopher Fang-Yen[a,1], Leon Avery[b], and Aravinthan D. T. Samuel[a]

[a]Department of Physics, Harvard University, 17 Oxford Street, Cambridge, MA 02138; and [b]Department of Molecular Biology, University of Texas Southwestern Medical Center, 5323 Harry Hines Boulevard, Dallas, TX 75390-9148

Edited by Martin Chalfie, Columbia University, New York, NY, and approved October 2, 2009 (received for review April 16, 2009)

Caenorhabditis elegans **is a filter feeder: it draws bacteria suspended in liquid into its pharynx, traps the bacteria, and ejects the liquid. How pharyngeal pumping simultaneously transports and filters food particles has been poorly understood. Here, we use high-speed video microscopy to define the detailed workings of pharyngeal mechanics. The buccal cavity and metastomal flaps regulate the flow of dense bacterial suspensions and exclude excessively large particles from entering the pharynx. A complex sequence of contractions and relaxations transports food particles in two successive trap stages before passage into the terminal bulb and intestine. Filtering occurs at each trap as bacteria are concentrated in the central lumen while fluids are expelled radially through three apical channels. Experiments with microspheres show that the** ***C. elegans*** **pharynx, in combination with the buccal cavity, is tuned to specifically catch and transport particles of a size range corresponding to most soil bacteria.**

filter feeding | pharyngeal pumping | pharynx

The *Caenorhabditis elegans* pharynx is a double-bulbed neuromuscular tube connecting the stoma and intestine (Fig. 1*A*). In the anterior procorpus and anterior isthmus, the apices of the triradiate lumen end in narrow channels (1). The radially oriented pharyngeal muscles drive two stereotyped motions: pharyngeal pumping and isthmus peristalsis (Fig. 1 *B–D*) (2). Pumping consists of two phases: (*i*) contraction of the pharyngeal muscle, which opens the pharyngeal lumen and draws in suspended bacteria, and (*ii*) relaxation, which rapidly closes the lumen. Relaxation is key to filtering because closure of the lumen ejects fluids while food particles remain trapped in the pharynx (2). Isthmus peristalsis consists of an anterior-to-posterior wave of transient contraction that carries bacteria from the anterior isthmus to the grinder in the terminal bulb, which crushes food before it enters the intestine.

Here, we show how pharyngeal pumping simultaneously filters bacteria and transports them from the stoma to the isthmus. These mechanisms have been poorly understood because pharyngeal relaxation is too rapid to be resolved by eye or standard video imaging. The feeding mechanisms of all animals on the size scale of *C. elegans* must solve a time-reversal problem posed by low-Reynolds number hydrodynamics (3, 4). That is, if the motions of the pharynx during relaxation are the reverse of those during contraction, no net transport would occur: bacteria that enter the *C. elegans* pharynx during contraction would be regurgitated during relaxation (3). Proposed mechanisms of pharyngeal transport and filtering have included anterior-to-posterior peristalsis of the procorpus during relaxation (5), trapping of bacteria by the pharyngeal lumen (3), and active regulation of bacterial flow by the metastomal flaps, which are cuticular projections in the buccal cavity (stoma) (5). Filamentous cuticular structures between the metacorpus and isthmus have been suggested to act as a "sieve" (1). Previous studies of imaging pharyngeal pumping (5) have been unable to test these mechanisms because they were limited by relatively low frame rates (24–60 frames per second) and the use of uncoordinated mutants, in which pharyngeal behaviors may not be identical to that of wild-type worms. In this work, we use high-speed imaging at 1,000 frames per second to observe motions of the pharyngeal muscles and ingested bacteria in wild-type animals.

Results

The Pharynx Traps Bacteria in Two Successive Stages. In our high-speed imaging experiments, N2 (Bristol) strain worms were imaged at 1,000 frames per second by Nomarski differential interference contrast (DIC) microscopy (6) during feeding on *Escherichia coli* OP50 bacteria or polystyrene beads. In our recordings, the motions of the pharyngeal muscles, bacteria, and stoma structures during pharyngeal pumping were clearly resolved (Fig. 2 and Movies S1–S7). We recorded high-speed video sequences from adults and animals of all larval stages (L1–L4). The following observations apply to all recordings.

We found that the pharynx traps bacteria in two stages. The pharynx first ingests particles through the stoma and traps them in the anterior procorpus. On the subsequent pump cycle, the pharynx transfers particles from the anterior procorpus to the anterior isthmus (Fig. 2 and Movies S1–S7).

Pharyngeal contraction lasted 145 ± 32 ms (mean ± SD) in young adults and was monitored by observing the movement of particles in the corpus. At the onset of relaxation—also the moment of maximum contraction—particles reversed direction and began to move anteriorly. We found that the anterior tip of the procorpus relaxed before the remainder of the corpus, creating a constriction immediately posterior to the base of the stoma (Fig. 2). Corpus relaxation, which lasted 35 ± 7 ms (mean ± SD), pushed particles in the corpus anteriorly toward this constriction, where they were trapped. Thus, the anterior tip of the procorpus works as a valve that prevents regurgitant flow of bacteria out of the pharynx. Relaxation of the anterior tip of the procorpus may involve the selective relaxation of a subcompartment of the pm3 muscles (1).

We found that the onset of isthmus contraction was delayed relative to the onset of corpus contraction, as previously reported (3). Anterior isthmus contraction in adults began 73 ± 36 ms (mean ± SD) after the onset of corpus contraction. Particles were observed to reach the anterior isthmus by either of two paths. The majority of particles were first trapped in the anterior procorpus, then relayed to the isthmus upon the subsequent pharyngeal pump cycle (Fig. 3). Some particles that entered the pharynx relatively early during the contraction phase bypassed the procorpus trap and were trapped directly in the anterior isthmus.

Particle trapping in the anterior isthmus is highly analogous to trapping in the procorpus. Anterior isthmus contraction drew particles from the corpus into the isthmus. Corpus relaxation, which

Author contributions: C.F.-Y., L.A., and A.D.T.S. designed research; C.F.-Y. performed research; C.F.-Y. analyzed data; and C.F.-Y., L.A., and A.D.T.S. wrote the paper.

The authors declare no conflict of interest.

This article is a PNAS Direct Submission.

[1]To whom correspondence should be addressed. E-mail: fangyen@fas.harvard.edu.

This article contains supporting information online at www.pnas.org/cgi/content/full/0904036106/DCSupplemental.

PHYSIOLOGY

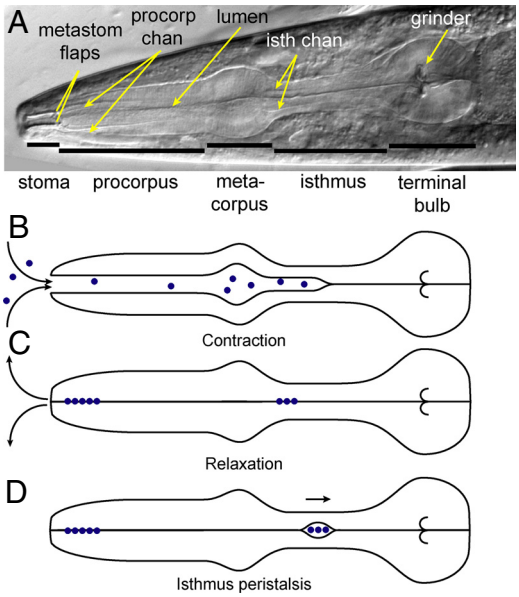

Fig. 1. Pharyngeal anatomy and behavior. (*A*) Annotated DIC image of anterior of adult worm (field of view, 177 μm × 57 μm). The corpus includes the procorpus and metacorpus. Intestine is posterior to the terminal bulb. (*B* and *C*) Pharyngeal pumping. Contraction of pharyngeal muscle draws fluid containing suspended food particles (dots) into pharyngeal lumen. Relaxation ejects fluids while trapping particles. Curved arrows indicate flow of fluids. (*D*) Isthmus peristalsis carries food from anterior isthmus to terminal bulb and intestine.

preceded isthmus relaxation, created a constriction near the boundary between the metacorpus and isthmus. Particles in the contracted anterior isthmus were pushed anteriorly against this constriction during isthmus relaxation, much as particles in the procorpus were trapped by the constriction at the anterior tip of the procorpus during corpus relaxation.

Fig. 3 describes the longitudinal positions of five bacteria in an adult worm during one cycle of pharyngeal pumping (Movie S4). For this cycle, bacteria 1 and 2 were initially outside the buccal cavity, bacteria 3 and 4 were trapped in the anterior procorpus, and bacterium 5 was trapped in the anterior isthmus trap. At the end of the pharyngeal pump, bacteria 1 and 2 had been transported to the anterior procorpus trap, and bacteria 3–5 were in the anterior isthmus trap. Peak velocities for bacteria 1–4 in the corpus during contraction were in the range of 2.7–3.7 mm/s. During relaxation, peak velocities for bacteria 1 and 2 in the corpus were 3.8 and 4.8 mm/s, respectively.

Pharyngeal transport of food particles functions in the same way in all larval stages as in adults. We did notice a gradual increase in the duration of both corpus and isthmus contraction during development. In Table S1, we summarize the data from timing of corpus contraction and relaxation, isthmus contraction and relaxation, delay between corpus and isthmus contraction, and overall pump period for larval and adult worms.

We asked how the duration of pharyngeal contractions and relaxations varies with the period of pharyngeal pumping. We found that the duration of corpus contraction was correlated with pump period ($R^2 = 0.678$; $P < 10^{-5}$; Fig. S1). We did not find significant correlations between corpus/isthmus relaxation times and pump period or between isthmus contraction time and pump period (Fig. S1). These results suggest that the rate of corpus contraction may be under active control in a manner correlated with the overall level of pharyngeal excitation, but relaxation rates may reflect the passive relaxation of the pharyngeal muscles, and are therefore independent of the pharyngeal pumping rate.

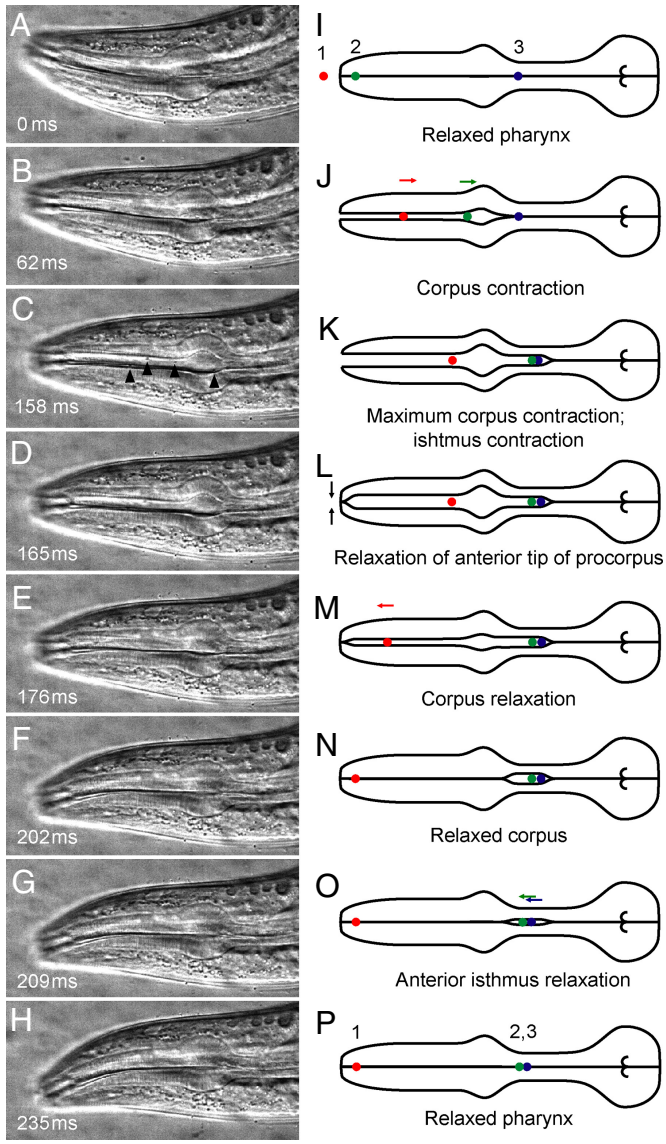

Fig. 2. High-speed video imaging of pharyngeal pumping. (*A–H*) Frames from high-speed video sequence showing movements of pharyngeal muscles and 0.75-μm polystyrene particles during pharyngeal pumping in adult worm (field of view, 136 μm × 65 μm). Black triangles in *C* indicate several particles. (*I–P*) Corresponding illustrations showing initial, intermediate, and final positions of three representative particles labeled 1 (red), 2 (green), and 3 (blue). During one cycle of contraction and relaxation, particle 1 has been transported from outside the pharynx to the anterior procorpus trap. Particle 2 has been transported from the anterior procorpus trap to the anterior isthmus trap. Particle 3 remains in the anterior isthmus trap. Full video sequence is available in Movie S1.

The Pharynx Traps Bacteria via a Radial Filtering Mechanism. Having established the patterns of pharyngeal movements and pathways of particle transport, we next addressed how the pharynx filters particles from fluids. In the anterior procorpus and anterior isthmus, but not elsewhere in the pharynx, the radii of the Y-shaped pharyngeal lumen end in apical channels. The apical channels in the procorpus and isthmus channels extend posteriorly from the buccal cavity and metacorpus, respectively (1) (Figs. 1 and 4*A*). The presence of these channels in the same locations as where particle trapping occurs suggests that they involved in trapping. It has been suggested that the channels allow fluid flow in and out of the pharynx (7), but a specific role of the channels in food filtering has not been described.

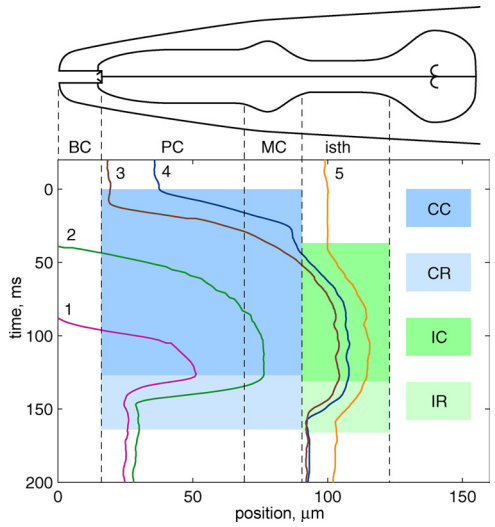

Fig. 3. Trajectories of five bacteria during one pharyngeal pump cycle in an adult worm. BC, buccal cavity; PC, procorpus; MC, metacorpus; isth, isthmus. Shaded regions indicate timing of different pumping phases. CC, corpus contraction (0–127 ms); CR, corpus relaxation (127–164 ms); IC, isthmus contraction (36–132 ms); IR, isthmus relaxation (132–166 ms). Positions of bacteria are measured along approximate centerline of pharynx with zero at tip of nose (see *Materials and Methods*). Time denoted relative to onset of corpus contraction. Pumping period for this video sequence was $t = 200$ ms. Corresponding video can be found in Movie S4.

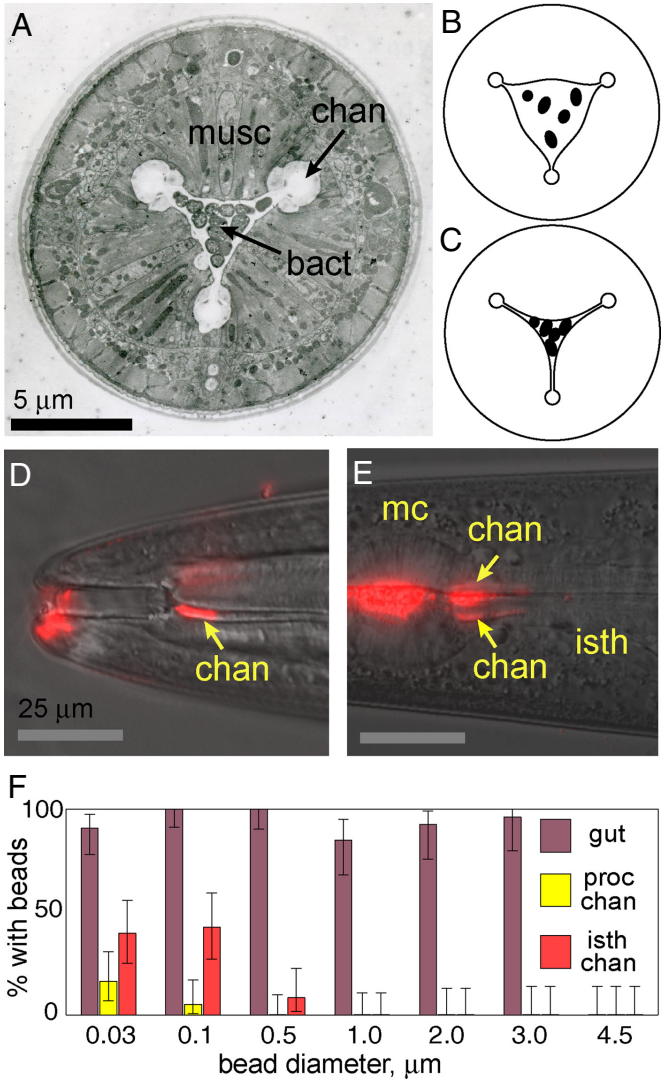

Fig. 4. Particle filtering. (*A*) Electron micrograph cross-section of pharynx anterior procorpus containing bacteria. musc, muscles; chan, channels; bact, trapped bacteria. (*B*) Illustration of cross-section of contracted pharynx containing bacterial suspension. (*C*) Illustration of cross-section after relaxation. Bacteria are trapped; fluid has flowed radially into channels. (*D*) Overlay of DIC image and fluorescence image from worm incubated with 0.03-μm-diameter red fluorescent beads. Beads aggregated in procorpus channels. Ventral channel (arrow) shown; subdorsal channels are out of focus in this image. Beads also present at anterior tip of worm. (*E*) Overlay of DIC image and fluorescence image from worm incubated with 0.1-μm-diameter red fluorescent beads. mc, metacorpus; isth, isthmus. Beads have aggregated in the anterior isthmus channels (arrows) and in the pharyngeal lumen. (*F*) Size-dependent accumulation of fluorescent beads in pharyngeal channels and gut. Fraction of worms positive for beads in anterior procorpus channels, anterior isthmus channels, or intestinal lumen for various bead diameters. Number of worms $n \geq 33$ for 0.03- to 1-μm beads, $n \geq 25$ for 2- to 4.5-μm beads. Error bars indicate 95% confidence intervals for true mean.

In our video sequences, we observed that bacteria were confined to the central lumen during both contraction and relaxation phases. We also observed that the outer boundary of the central lumen and inner boundary of the apical channels are separated by a small gap (1–2 μm) in which bacteria were never seen (Movie S6). Based on these observations, we hypothesized that the pharynx functions as a radial filter: bacteria are trapped in the central lumen while fluid is expelled radially outward into the apical channels (Fig. 4 *B* and *C*). The channels provide a path for fluids to exit the pharynx through the stoma. For radial filtering to work, it is important that throughout the pumping process the passage separating the central lumen and apical channels remains narrower than the size of food particles (≈0.5 μm for *E. coli* OP50; see Table S2). Indeed, in electron micrographs of the anterior procorpus in a worm with a pharynx full of bacteria (Fig. 4*A*), the central lumen is separated from the apical channels by a constriction ≈0.1–0.2 μm wide (note that shrinkage from fixation, dehydration, and embedding is minor, typically 5–10%; ref. 8). The cuticle layer lining the central lumen is thickest near the constriction between the central lumen and apical channels, which may serve as a reinforcement to prevent pharyngeal muscle contraction from widening the constriction. Consistent with this idea, the channels do not appear to change size or shape during pharyngeal contraction and relaxation (Movie S6).

Our model of a size-dependent radial filter implies that the gap between the central lumen and apical channels defines a minimum particle size for efficient filtering. In other words, sufficiently small particles should to be able to enter the channels, and larger particles should be excluded. To evaluate the size dependence of particle transport in the pharynx, we fed worms suspensions of red fluorescent latex microspheres of diameters 0.03, 0.1, 0.5, and 1.0 μm and nonfluorescent polystyrene beads of diameters 2.0, 3.0, and 4.5 μm. The beads tended to adhere to all surfaces of the worm, including the inner surface of the pharyngeal lumen and apical channels, and thus could be used for tracing where particles of a given size could go (Fig. 4 *D* and *E*). After 2 h, we manually scored each worm for the presence of beads in the corpus lumen, procorpus channels, isthmus lumen, anterior isthmus channels, and gut (Table S3) by using fluorescence and DIC microscopy.

Fig. 4*F* shows the results for bead accumulation in anterior procorpus and anterior isthmus apical channels of young adult worms. We found that 0.03- to 0.1-μm-diameter beads could enter the procorpus channels, whereas beads of diameters 0.5 μm and greater were excluded; 0.03- to 0.1-μm-diameter beads and, to a lesser extent, 0.5-μm-diameter beads, could enter the isthmus

PHYSIOLOGY

channels, whereas beads of diameters 1.0 μm and greater were excluded. These results show that size filtering occurs between the central lumen and apical channels, consistent with our radial filtering model.

Buccal Cavity and Associated Structures Exclude Large Particles and Regulate Bacteria Flow. In addition to examining the lower size limit for particle filtering, we also investigated the upper size limit by testing the ability of worms to transport relatively large particles of diameters 2–4.5 μm (Fig. 4*F*) into the pharynx and intestine. We found that young adult worms can transport microspheres of diameters up to and including 3 μm, whereas beads of diameter 4.5 μm did not enter the buccal cavity. Beads that did enter the pharynx were transported through the isthmus and terminal bulb into the intestine. The polystyrene beads appeared to be unaffected by their passage through the grinder.

We investigated the possible functions of the metastomal flaps, three cuticular projections at the base of the buccal cavity (9). Seymour et al. (5) reported that the metastomal flaps actively open and close during pharyngeal pumping. However, in 10 recordings from different worms in which the metastomal flaps were clearly resolved, we observed no movement of the flaps relative to the buccal cavity during pumping or between pumps. Our observations suggest a different role for the metastomal flaps. During feeding in a dense bacterial suspension (Movie S6), the stoma often becomes tightly packed with bacteria. This packing, visible in low-speed recordings, was interpreted previously as resulting from an active closure of the metastomal flaps, completely preventing bacteria from entering the pharynx (3, 5). Our high-speed recordings show that bacteria continue to filter through the metastomal flaps during contraction, albeit at a reduced rate. It is likely that the digestive system has a maximum food intake rate. The metastomal flaps might passively regulate the flow of bacteria to below this level. In dilute suspensions, the metastomal flaps did not appear to impede the flow of bacteria into the pharynx. The metastomal flaps may also play some role in prefiltering large particles (Movie S7).

Discussion

Our work resolves several longstanding questions regarding how *C. elegans* catches food. We show that transfer and trapping of particles are performed by analogous patterns of contractions and relaxations in the procorpus and anterior isthmus. The motions of both the corpus and isthmus during contraction and relaxation are each highly nonreciprocal because of the early relaxations of the lumen anterior to each trap. The pharynx can thus be seen as a two-chambered pump, with each chamber equipped with a valve to prevent regurgitant particle flow.

We have described a mechanism of filter feeding based on outward radial flow of fluids from the central lumen to the apical channels. We show that the pharynx, in combination with the buccal cavity, which excludes excessively large particles, can be considered a mechanical "band pass" filter, efficiently transporting particles of a size range of ≈0.5–3 μm in young adults. This range includes the sizes of many bacterial strains isolated from the soil (Table S2) (3) and is likely to include the size range of bacteria consumed by *C. elegans* in its natural habitats.

Pharyngeal pumping persists when the entire pharyngeal nervous system has been destroyed by laser ablation, but the pumping that results is abnormal and inefficient (10). The majority of pharyngeal neurons are likely to exert effects not readily apparent by visual observation (11). High-speed imaging of pharyngeal mechanics may provide a foundation for more detailed investigations into how the pharyngeal nervous system modulates pharyngeal behavior in *C. elegans* and other nematodes (12).

Materials and Methods

N2 (Bristol) worms were grown at 20 °C on NGM plates containing OP50 *E. coli* by using standard methods (6) and were synchronized by using hypochlorite bleaching when necessary. For high-speed imaging experiments, several worms and a small amount (≈2–4 μL) of *E. coli* OP50 bacteria were transferred to an agarose pad (2% wt/vol agarose in M9 or NGM buffer) on a microscope slide. We recorded high-speed image sequences from a total of 12 L1 larvae, 14 L2 larvae, 13 L3 larvae, 12 L4 larvae, and 45 adults. For high-speed imaging of worms feeding on beads, we added 2 μL of a 1% (vol/vol) solution of polystyrene beads (Polysciences) of various diameters, diluted in NGM buffer to 0.1% vol/vol. The agar pad was covered by a coverslip and sealed with wax to minimize dehydration. Worms were allowed to accommodate to the pad for 30–60 min before being imaged on an inverted microscope (Nikon TE2000) using 40×, 60×, or 100× oil immersion objectives. We recorded image sequences of 3- to 4-s duration at 1,000 frames per second by using Photron (1024-PCI; 1024 × 1024 pixels; Photron) or Phantom (V9; 1632 × 1200 pixels; Vision Research) high-speed video cameras.

We viewed image sequences frame by frame and manually recorded the frame numbers corresponding to the start of corpus contraction, start of corpus relaxation, end of corpus relaxation, start of isthmus contraction, start of isthmus relaxation, and end of isthmus relaxation in recordings of two to four pump cycles from all image sequences in which both corpus and isthmus pumping were clearly visible.

To trace positions of particles during pharyngeal pumping, we manually tracked (*i*) the positions of each particle of interest and (*ii*) several reference points along the center of the pharyngeal lumen: from the base of the stoma to the midprocorpus, center of the metacorpus, center of the isthmus, and end of the isthmus. For each frame, we calculated a cubic smoothing spline to the reference points to approximate the centerline of the pharyngeal lumen. Each particle's position along the length of the pharynx was calculated as the path length along the spline from the anterior tip of the worm to the point on the spline curve closest to the particle in each image.

All image adjustments, reviewing, analyses, calculations, and conversions were performed by using custom software written in MATLAB (MathWorks).

For the experiments described in Fig. 4 *D–F*, 10 μL of a 2.5% vol/vol suspension of red fluorescent polystyrene microspheres (Sigma–Aldrich) or nonfluorescent polystyrene microspheres (Polysciences) was spread over 6-cm plates containing 5 mL of 2% agarose and 200 mM sorbitol (a nonionic solute used to reducing the clumping of beads). We picked young adult N2 worms from NGM plates into the bead-containing plates and incubated at 20 °C for 2 h. For imaging, worms were transferred to pads containing 2% agarose, 200 mM sorbitol, and 3 mM sodium azide as anesthetic. The pads were covered with cover glass, sealed with wax, and imaged at 40× to 100× magnification by using DIC and fluorescence optics (with Texas Red/mCherry filter sets) on an inverted microscope.

ACKNOWLEDGMENTS. We thank David H. Hall (Albert Einstein College of Medicine, Bronx, NY) for unpublished electron micrographs, David Weitz (Harvard University, Cambridge, MA), L. Mahadevan (Harvard University, Cambridge, MA), H. Sebastian Seung (Massachusetts Institute of Technology, Cambridge, MA), and Michael S. Feld (Masschusetts Institute of Technology, Cambridge, MA) for the loan of high-speed cameras, and Howard Stone (Harvard University, Cambridge, MA) for helpful suggestions. This work was supported by the National Science Foundation.

1. Albertson DG, Thomson JN (1976) The pharynx of *Caenorhabditis elegans*. *Philos Trans R Soc Lond B Biol Sci* 275:299–325.
2. Avery L (1993) The genetics of feeding in *Caenorhabditis elegans*. *Genetics* 133:897–917.
3. Avery L, Shtonda BB (2003) Food transport in the *C elegans* pharynx. *J Exp Biol* 206:2441–2457.
4. Purcell EM (1977) Life at low Reynolds number. *Am J Phys* 45:3–11.
5. Seymour MK, Wright KA, Doncaster CC (1983) The action of the anterior feeding apparatus of *Caenorhabditis elegans* (Nematoda, *Rhabditida*). *J Zool* 201:527–539.
6. Sulston JE, Hodgkin JA (1988) in *The Nematode Caenorhabditis elegans*, ed Wood WB (Cold Spring Harbor Laboratory Press, Cold Spring Harbor, NY), pp 587–606.
7. White J (1988) in *The Nematode Caenorhabditis elegans*, ed Wood WB (Cold Spring Harbor Laboratory Press, Cold Spring Harbor, NY), pp 587–606.
8. Hayat MA (2000) *Principles and Techniques of Electron Microscopy: Biological Applications* (Cambridge Univ Press, Cambridge, UK).
9. Wright KA, Thomson JN (1981) The buccal capsule of *Caenorhabditis elegans* (Nematoda, *Rhabditoidea*) - an ultrastructural study. *Can J Zool* 59:1952–1961.
10. Avery L, Horvitz R (1989) Pharyngeal pumping continues after laser killing of the pharyngeal nervous system of *C. elegans*. *Neuron* 3:473–485.
11. Avery L (1993) Motor neuron M3 controls pharyngeal muscle relaxation timing in Caenorhabditis elegans. *J Exp Biol* 175:283–297.
12. Chiang JT, Steciuk M, Shtonda B, Avery L (2006) Evolution of pharyngeal behaviors and neuronal functions in free-living soil nematodes. *J Exp Biol* 209:1859–1873.